High Real-Space Resolution Measurement of the Local Structure of $Ga_{1-x}In_xAs$ Using X-Ray Diffraction

V. Petkov,[1] I-K. Jeong,[1] J. S. Chung,[1] M. F. Thorpe,[1] S. Kycia,[2] and S. J. L. Billinge[1]
[1]*Department of Physics and Astronomy and Center for Fundamental Materials Research, Michigan State University, East Lansing, Michigan 48824-1116*
[2]*Cornell High Energy Synchrotron Source, Cornell University, Ithaca, New York 14853*
(Received 7 June 1999)

High real-space resolution atomic pair distribution functions PDFs from the alloy series $Ga_{1-x}In_xAs$ have been obtained using high-energy x-ray diffraction. The first peak in the PDF is resolved as a doublet due to the presence of two nearest neighbor bond lengths, Ga-As and In-As, as previously observed using x-ray absorption fine structure. The widths of nearest, and higher, neighbor PDF peaks are analyzed by separating the broadening due to static atom displacements from the thermal motion. The PDF peak width is 5 times larger for distant atomic neighbors than for nearest neighbors. The results are in agreement with model calculations.

PACS numbers: 61.66.Dk, 61.43.Dq, 61.72.Dd

The average atomic arrangement of crystalline semiconductor alloys is usually obtained from the position and intensities of the Bragg peaks in a diffraction experiment [1], and the actual nearest neighbor and sometimes next nearest neighbor distances for various pairs of atoms by XAFS measurements [2]. In this Letter, we show how high-energy x-ray diffraction and the resulting high-resolution atomic pair distribution functions PDFs can be used for studying the local atomic arrangements in $Ga_{1-x}In_xAs$ alloys. We show that the first peak in the PDFs can be resolved as a doublet and, hence, the mean position and also the widths of the Ga-As and In-As bond length distributions determined. The detailed structure in the PDF can be followed out to very large distances and the widths of the various peaks obtained. We use the concentration dependence of the peak widths to separate the broadening due to static atom displacements from the thermal broadening. At large distances the static part of the broadening is shown to be up to 5 times larger than it is for nearest neighbor pairs. Using a simple valence force field model, we get good agreement with the experimental results.

Ternary semiconductor alloys, in particular $Ga_{1-x}In_xAs$, have technological significance because they allow important properties, such as band gaps, to be tuned continuously between the two end points by varying the composition x. Surprisingly, there is no complete experimental determination of the microscopic structure of these alloys. On average, both GaAs and InAs form in the zinc-blende structure where Ga or In and As atoms occupy two interpenetrating face-centered-cubic lattices and are tetrahedrally coordinated to each other [1]. However, both extended x-ray absorption fine structure (XAFS) experiments [2] and theory [3] have shown that Ga-As and In-As bonds do not take some average value but remain close to their *natural* lengths of $L^0_{\text{Ga-As}} = 2.437$ Å and $L^0_{\text{In-As}} = 2.610$ Å in the alloy. Because of the two different bond lengths present, the zinc-blende structure of $Ga_{1-x}In_xAs$ alloys becomes locally distorted. A number of authors [2–5] have proposed distorted local structures, but there have been limited experimental data available to date. The fully distorted structure is a prerequisite as an input for accurate band structure and phonon dispersion calculations [6].

The technique of choice for studying the local structure of semiconductor alloys has been XAFS [2,5]. However, XAFS provides information only about the immediate atomic ordering (first and sometimes second coordination shells) and all longer-ranged structural features remain hidden. To remedy this shortcoming, we have taken the alternative experimental approach of obtaining high-resolution PDFs of these alloys from high-energy x-ray diffraction data.

The PDF is the instantaneous atomic density-density correlation function which describes the local arrangement of atoms in a material [7]. The PDF, $G(r)$, is the sine Fourier transform of the experimentally observable total structure factor, $S(Q)$, where Q is the magnitude of the wave vector, given by

$$G(r) = \frac{2}{\pi} \int_0^{Q_{\max}} F(Q) \sin Qr \, dQ \,, \qquad (1)$$

with $F(Q) = Q[S(Q) - 1]$. The total structure factor, $S(Q)$, is the normalized scattered intensity from the powder sample.

PDF analysis yields the real local structure, whereas an analysis of the Bragg scattering alone yields the average crystal structure. Determining the PDF has been the approach of choice for characterizing glasses, liquids, and amorphous materials for a long time [8]. However, its widespread application to study *crystalline* materials has been relatively recent [9]. Very high real-space resolution is required to differentiate the distinct Ga-As and In-As bond lengths present in $Ga_{1-x}In_xAs$. High real-space resolution is obtained by measuring $S(Q)$ to a very high value of Q ($Q_{\max} \geq 40$ Å^{-1}). An indium neutron absorption resonance rules out neutron measurements in the

 © 1999 The American Physical Society

$Ga_{1-x}In_xAs$ system. We therefore carried out x-ray powder diffraction measurements. To access Q values in the vicinity of 40–50 $Å^{-1}$ it is necessary to use x rays with energies $\geq$50 keV. The experiments were carried out at the A2 24 pole wiggler beam line at Cornell High Energy Synchrotron Source (CHESS), which is capable of delivering intense x rays of energy 60 keV. Six powder samples of $Ga_{1-x}In_xAs$, with $x = 0.0$, 0.17, 0.5, 0.67, 0.83, and 1.0, were measured. The samples were made by standard methods and the details of the sample preparation will be reported elsewhere [10]. All measurements were done in symmetric transmission geometry at 10 K. The relative intensities of the Bragg peaks compare well with those expected from the crystal structure, suggesting that the samples are free of any significant texture. Low temperature was used to minimize thermal vibration in the samples, and hence to increase the sensitivity to static atomic displacements. A double crystal Si(111) monochromator was used. Scattered radiation was collected with an intrinsic germanium detector connected to a multichannel analyzer. The elastic component was separated from the incoherent Compton scattering before data analysis [10]. Several diffraction runs were conducted with each sample, and the resulting spectra averaged to improve the statistical accuracy. The data were normalized for flux, corrected for background scattering, detector deadtime and absorption, and divided by the average form factor to obtain the total structure factor, $S(Q)$ [7,8,11], using the program RAD [10,12]. Experimental reduced structure factors, $F(Q)$, are shown in Fig. 1. The corresponding reduced PDFs, $G(r)$, are shown in Fig. 2. The data for the Fourier transform were terminated at $Q_{max} = 45$ $Å^{-1}$ beyond which the signal to noise ratio became unfavorable. This is a very high momentum transfer for x-ray diffraction measurements. For comparison, Q_{max} from a Cu K_α x-ray tube is less than 8 $Å^{-1}$.

Significant Bragg scattering (well-defined peaks) are immediately evident in Fig. 1 up to $Q \sim 35$ $Å^{-1}$ in the end members, GaAs and InAs. This implies that the samples have long range order and that there is little positional disorder (dynamic or static) on the atomic scale. The Bragg peaks disappear at much lower Q values in the alloy data: the samples are still long-range ordered but they have significant local positional disorder. At high-Q values, oscillating diffuse scattering is evident. This has a period of $2\pi/2.5$ $Å^{-1}$ and contains information about the shortest atomic distances in $Ga_{1-x}In_xAs$ alloys seen as a sharp first peak in $G(r)$ at 2.5 Å (see Fig. 2). In the alloys, this peak is split into a doublet as is clearly evident in Fig. 2; with a shorter Ga-As bond and a longer In-As bond. This peak is shown on an expanded scale in the inset to Fig. 3 for all the compositions measured. We determined the positions of the two subcomponents of the first PDF peak, i.e., the mean Ga-As and In-As bond lengths, and the results are shown in Fig. 3. Also shown is the room temperature result previously obtained in the XAFS study of Mikkelson and Boyce [2]. There is clearly good agreement. The PDF-based bond lengths are shifted to smaller lengths by about 0.012 Å since our data were measured at 10 K, whereas the XAFS experiments were at room temperature. The nearest neighbor peak is the only peak which is sharp in the experimental PDFs, as can be seen in Fig. 2. From the second-neighbor onwards the significant atomic displacements in the alloy samples result in broad atom-pair distributions without any resolvable splitting. Model calculations show that this broadening is intrinsic and not due to any experimental limitations. The PDF peak widths in $Ga_{1-x}In_xAs$ were quantified by fitting individual peaks using Gaussians convoluted with sinc functions with FWHM 0.086 Å to account for the experimental resolution coming from the finite Q_{max}. At low r this was accomplished by fitting individual peaks. At high r where there is significant peak overlap a profile fitting regression program was used [13]. The resulting mean-square Gaussian standard deviations are shown in Fig. 4. One can see that the static contribution to the PDF peak width on 2nd and higher neighbors is up to 5 times larger than on the near neighbors. The peak width has a maximum at a composition $x = 0.5$ and affects the common (As) more than the mixed (metal) sublattice.

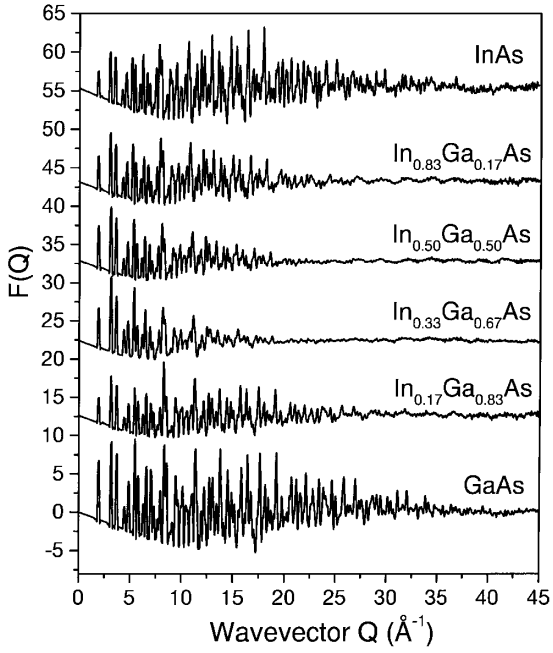

FIG. 1. The reduced structure factor, $F(Q)$, for $Ga_{1-x}In_xAs$ measured at 10 K for various concentrations.

In order to better understand these results, we have modeled to the static and thermal disorder in the alloy by using a Kirkwood potential [14]. The potential contains nearest neighbor bond stretching force constants α and force constants β that couple to the change in the angle between adjacent nearest neighbor bonds. We choose these parameters to fit the end members [3] with $\alpha_{Ga\text{-}As} = 96$ N/m, $\alpha_{In\text{-}As} = 97$ N/m, $\beta_{Ga\text{-}As\text{-}Ga} = \beta_{As\text{-}Ga\text{-}As} = 10$ N/m, and

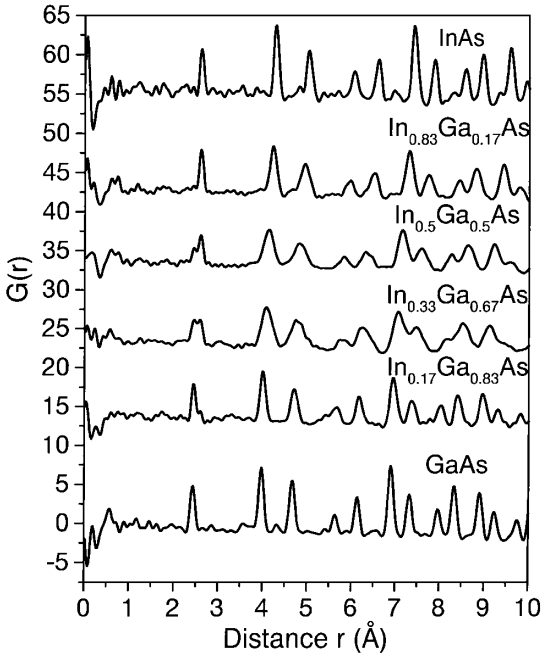

FIG. 2. The reduced PDF, $G(r)$, for $Ga_{1-x}In_xAs$ measured at 10 K for various concentrations.

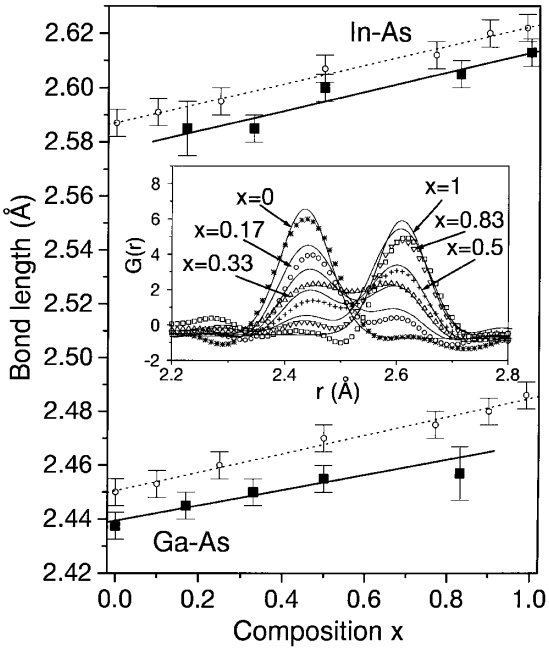

FIG. 3. Solid symbols: Ga-As and In-As bond lengths vs composition as extracted from the present PDFs. Open symbols: room-temperature XAFS results from Ref. 2. Inset: Split nearest neighbor PDF peak from the data (symbols) and the model (solid lines).

$\beta_{\text{In-As-In}} = \beta_{\text{As-In-As}} = 6$ N/m. The additional angular force constant required in the alloy is taken to be the geometrical mean, so that $\beta_{\text{Ga-As-In}} = \sqrt{(\beta_{\text{Ga-As-Ga}}\beta_{\text{In-As-In}})}$. We have constructed a series of cubic 512 atom periodic supercells in which the Ga and In atoms are distributed randomly according to the composition x. The system is relaxed using the Kirkwood potential to find the displacements from the virtual crystal positions. The volume of the supercell is also adjusted to find the minimum energy. Using this strained static structure, a dynamical matrix has been constructed, and the eigenvalues and eigenvectors found numerically. From this the Debye-Waller factors for all the individual atoms in the supercell can be found and hence the PDF of the model by including the Gaussian broadening of all the subpeaks, which is the correct procedure within the harmonic approximation [15]. The model PDF is plotted with the data in the inset to Fig. 3 and in Fig. 5. The agreement at higher r is comparable to that in the r range shown. All the individual peaks shown in the figures consist of many Gaussian subpeaks. The overall fit to the experimental $G(r)$ is excellent, and the small discrepancies in Fig. 5 between theory and experiment are probably due to small residual experimental errors. Note that in comparing with experiment, the theoretical PDF has been convoluted with a sinc function to incorporate the truncation of the experimental data at $Q_{\max} = 45$ Å. The technique discussed above could be extended using a better force constant model with more parameters, but does not seem necessary at this time.

The contributions from static displacements and thermal motion to the widths of the individual peaks in the reduced PDF act independently as expected and as confirmed by our supercell calculations described in the

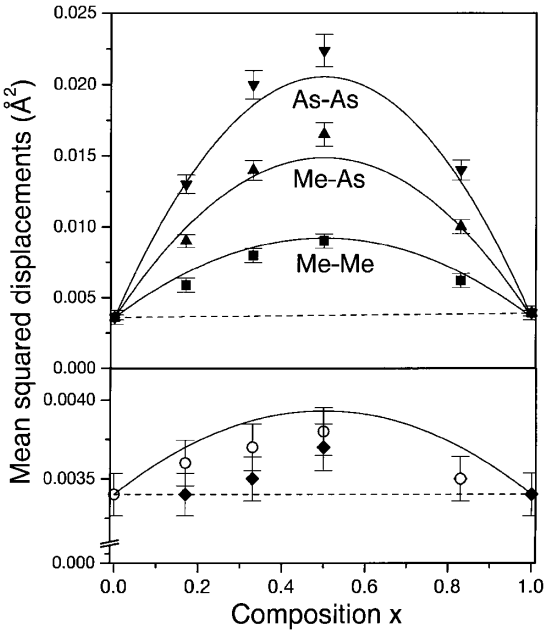

FIG. 4. Square of the PDF peak widths for far neighbors (top panel) and nearest neighbors (lower panel) separated by sublattice type. Symbols: values from the data. In the lower panel the open symbols are for the Ga-As bond and the closed symbols for the In-As bond. Solid lines: theory. See text for details. The mean-square static and thermal distortions are added. Here Me represents both the metals Ga and In, which behave in the same way. Note that the scale in the lower panel is expanded by a factor of 10 compared to the upper panel.

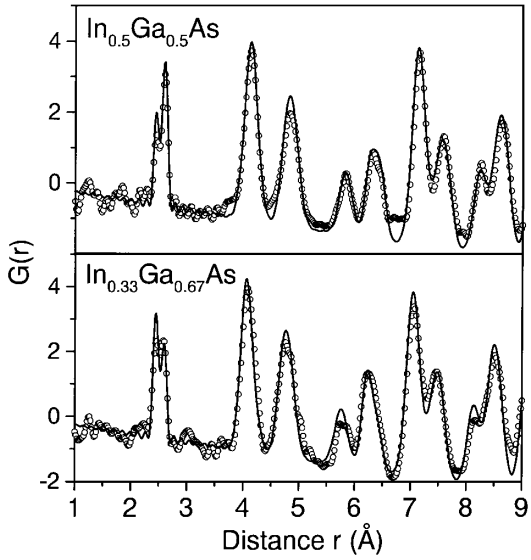

FIG. 5. Experimental (open circles) and theoretical (solid line) PDFs for $Ga_{1-x}In_xAs$ for concentrations $x = 0.5$ and $x = 0.33$.

previous paragraph. We therefore expect the squared width Δ to be a sum of the two parts. The thermal part σ is almost independent of the concentration, and we fit σ^2 by a linear function of the composition x between the two end points in Fig. 4. To better understand the strain, it is convenient to assume that all the force constants are the same and independent of chemical species. Then it can be shown [16] for any such model that

$$\Delta_{ij}^2 = \sigma_{ij}^2 + A_{ij}x(1 - x)(L_{\text{In-As}}^0 - L_{\text{Ga-As}}^0)^2, \quad (2)$$

where the subscripts ij refer to the two atoms that lead to a given peak in the reduced PDF. For the Kirkwood model the A_{ij} are functions of the ratio of force constants β/α only. It further turns out that the A_{ij} are independent of whether a site in one sublattice is Ga or In, so we will just refer to that as the metal site. By taking mean values from the force constants used in the simulation we find that $\beta/\alpha = 0.83$, and that for nearest neighbor pairs $A_{ij} = 0.0712$. For more distant pairs the motion of the two atoms becomes uncoupled so that $A_{ij} = A_i + A_j$, and we find that for the metal site $A_i = 0.375$ and for the As site $A_i = 1.134$. The validity of the approximation of using mean values for the force constants was shown to be accurate by calculating the model PDF for all compositions as described above and comparing to the prediction of Eq. (2) [16]. Equation (2) shows good agreement with the data for near and far neighbor PDF peaks, and for the different sublattices, over the whole alloy range, as shown in Fig. 4, using only parameters taken from fits to the end members. There is a considerably larger width associated with the As-As peak in Fig. 4 when compared to the Me-Me peak, because the As atom is surrounded by four metal cations, providing five distinct first-neighbor environments [4,5]. The theoretical curve in the lower panel of Fig. 4 is predicted to be the same for the Ga-As and the In-As bond length distribution, using the simplified approach. The Kirkwood model seems adequate to describe the experimental data at this time, although further refinement of the error bars may require the use of a better potential containing more parameters.

We would like to thank Rosa Barabash for discussions and help with the analysis of the static atom displacements, and Andrea Perez and the support staff at CHESS for help with data collection and analysis. This work was supported by DOE through Grant No. DE FG02 97ER45651. CHESS is operated by NSF through Grant No. DMR97-13424.

[1] R. W. G. Wyckoff, *Crystal Structures* (Wiley, New York, 1967), Vol. 1, 2nd ed.
[2] J. C. Mikkelson and J. B. Boyce, Phys. Rev. Lett. **49**, 1412 (1982); J. C. Mikkelsen and J. B. Boyce, Phys. Rev. B **28**, 7130 (1983).
[3] Y. Cai and M. F. Thorpe, Phys. Rev. B **46**, 15 879 (1992).
[4] J. L. Martins and A. Zunger, Phys. Rev. B **30**, 6217 (1984); M. C. Schabel and J. L. Martins, Phys. Rev. B **43**, 11 873 (1991).
[5] A. Balzarotti *et al.*, Phys. Rev. B **31**, 7526 (1985); H. Oyanagi *et al.*, Solid State Commun. **67**, 453 (1988).
[6] A. Zunger *et al.*, Phys. Rev. Lett. **65**, 353 (1990).
[7] B. E. Warren, *X-Ray Diffraction* (Dover, New York, 1990).
[8] Y. Waseda, *The Structure of Non-Crystalline Materials* (McGraw-Hill, New York, 1980).
[9] T. Egami, Mater. Trans. **31**, 163 (1990); T. Egami, in *Local Structure from Diffraction*, edited by S. J. L. Billinge and M. F. Thorpe (Plenum, New York, 1998), p. 1.
[10] I-K. Jeong, F. Mohiuddin-Jacobs, V. Petkov, and S. J. L. Billinge (unpublished).
[11] H. P. Klug and L. E. Alexander, *X-ray Diffraction Proceedures for Polycrystalline Materials* (Wiley, New York, 1974), 2nd ed.
[12] V. Petkov, J. Appl. Crystallogr. **22**, 387 (1989).
[13] Th. Proffen and S. J. L. Billinge, J. Appl. Crystallogr. **32**, 572 (1999).
[14] J. G. Kirkwood, J. Chem. Phys. **7**, 506 (1939).
[15] Jean S. Chung and M. F. Thorpe, Phys. Rev. B **55**, 1545 (1997); **59**, 4807 (1999); M. F. Thorpe *et al.*, in *Local Structure from Diffraction*, edited by S. J. L. Billinge and M. F. Thorpe (Plenum, New York, 1998), p. 157.
[16] J. S. Chung, R. I. Barabash, and M. F. Thorpe (unpublished).